Chapter 8
Surface Finishing Post-treatments for Additive Manufactured Metallic Components

T. S. N. Sankara Narayanan and Hyung Wook Park

8.1 Introduction

Additive manufacturing (AM) involves fabrication of numerous components by a layer-by-layer approach. AM processes assume significance due to their ability to fabricate thin lattice structures, struts and scaffolds with high material utility. Selective laser melting (SLM) and electron beam melting (EBM) are commonly employed for the fabrication of metallic components. One of the major limitations of components built by SLM and EBM is their higher surface roughness. Adherence of the partially melted particles, balling effect and stair case effect are the major reasons for the higher surface roughness [12, 43]. Many components involve complex shapes. Parts built away from the centre point of the build plate exhibit a higher surface roughness. Down-skin surfaces have a higher surface roughness than up-skin surfaces [12]. A higher surface roughness of the as-built AM part could deleteriously influence the mechanical properties, fatigue strength and corrosion resistance. The higher surface roughness of the AM parts restricts their use for the intended purpose and warrants suitable surface finishing post-treatments. Hence, the most important purpose of surface finishing post treatments is to reduce the surface roughness and to remove the partially melted particles present in the as-built AM parts. Surface finishing of AM components with a simple design can be easily accomplished. However, AM

T. S. N. Sankara Narayanan (✉) · H. W. Park
Department of Mechanical Engineering, Ulsan National Institute of Science and Technology (UNIST), UNIST-Gil 50, Eonyang-eup, Ulsan 689-798, Republic of Korea

H. W. Park
e-mail: hwpark@unist.ac.kr

Present Address:
T. S. N. Sankara Narayanan
Department of Analytical Chemistry, University of Madras, Guindy Campus, Chennai 600 025, India

parts with a complex design, internal surfaces, thin lattice structures, struts and scaffolds pose a tough challenge [52, 70]. A variety of surface finishing post-treatments are explored to decrease the surface roughness of AM parts [40, 41, 48, 56]. They can be broadly classified as (i) mechanical surface finishing methods; (ii) abrasive finishing methods; (iii) chemical and electrochemical processes; and (iv) laser and electron beam irradiation processes. This chapter aims to provide an outline of the ability of various surface finishing post-treatments to improve the surface finish of AM parts. The principle and mechanism of the treatment method, the beneficial effects induced by the treatment and the major limitations are highlighted.

8.2 Mechanical Surface Finishing Methods

8.2.1 Tumble/barrel Finishing

Tumble finishing (TF) or barrel finishing (BF) is a mechanical surface treatment process to improve surface finishing of metallic components. It involves tumbling or rotation of a barrel in which the parts to be treated and abrasive particles dispersed in a media are placed together. The friction between the surface being treated and the abrasive particles is responsible for the reduction in surface roughness. The extent of decrease in surface roughness is rather limited since the abrasive particles mainly remove the peaks while they have very little influence on the deep valleys. Boschetto et al. [9] have ascertained the suitability of BF for treating complex AM parts using a Ti6Al4V alloy impeller and an Inconel 718 alloy automotive exhaust manifold. The availability of limited space for the movement of the abrasive particles delays the speed of BF of the blades of the Ti6Al4V alloy impeller (Fig. 8.1a, b). The limited access for the abrasive particles on the angled internal surface limits the extent of surface finishing of the Inconel 718 alloy automotive exhaust manifold (Fig. 8.1c, d). Although BF has the advantage of treating many parts at the same time, the requirement of longer processing time (~48 h), wastage of the abrasive media, and problems in disposal are the major limitations in using them.

8.2.2 Finish Machining

Finish machining (FM) has been shown to decrease the surface roughness of SLM Inconel 718 alloy and 316L SS part by 90–96%. The extent of deformation induced by FM is very high, which enables grain refinement. In addition, the deformation helps to reduce the surface and sub-surface porosities. The strain hardening induced by FM increased the hardness and wear resistance and, decreased the risk of fatigue failure [37–39]. FM is not considered to be suitable for AM parts with complex shapes [38]. The depth of material removal during FM assumes significance as it
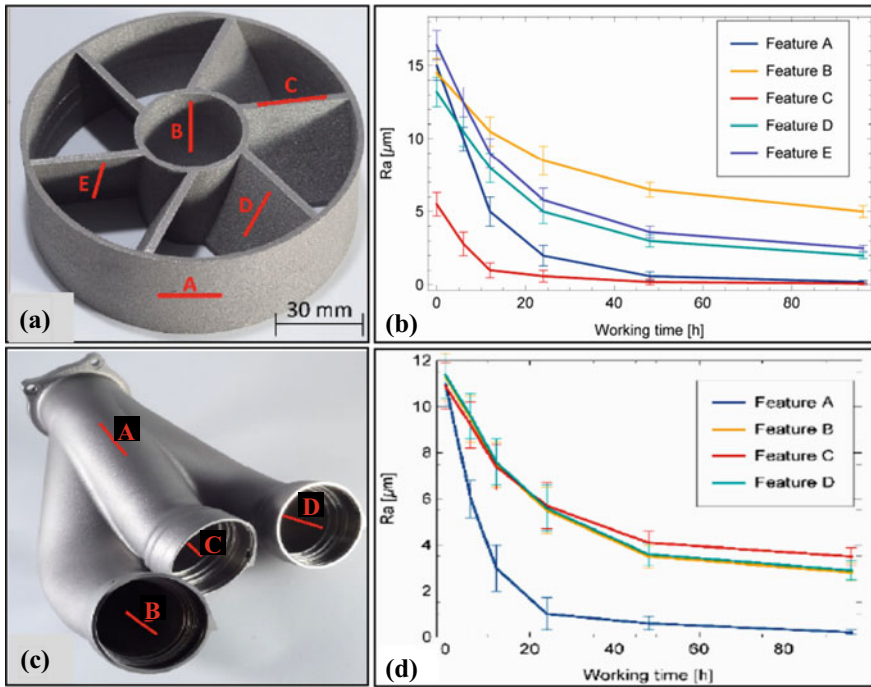
Fig. 8.1 Photographic images of SLM **a** Ti6Al4V impeller and **c** Inconel 718 alloy automotive exhaust manifold showing the regions at which the surface roughness was measured after BF; **b**, **d** Decrease in average surface roughness of these components after BF, measured as a function of time (Reprinted from, Boschetto et al. [9], under Creative Commons Attribution License)

could expose porosities and other defects from sub-surfaces. FM of EBM Ti6Al4V alloy parts to a depth of 1.00 mm bring out lack of fusion (LOF) defects to the top surface while those machined to a depth of 0.50 mm was free of such defects (Fig. 8.2). Although FM to a higher depth could offer considerable improvement in fatigue life by removing most of the pores and defects, such approach defeats the main principles of AM in terms of material utility with minimal wastage [17].

8.2.3   Blasting

Blasting involves propelling of abrasive particles (quartz sand, glass bead, alumina) on the surface to be treated under high pressure. Air pressure, stand-off distance, size and shape of the abrasive particles, angle of impingement and time are the main process variables. Blasting reduces the surface roughness, improves the surface integrity, increases the hardness and induces compressive residual stress. Micro-forming of the surface during blasting is responsible for smoothening of the surface.
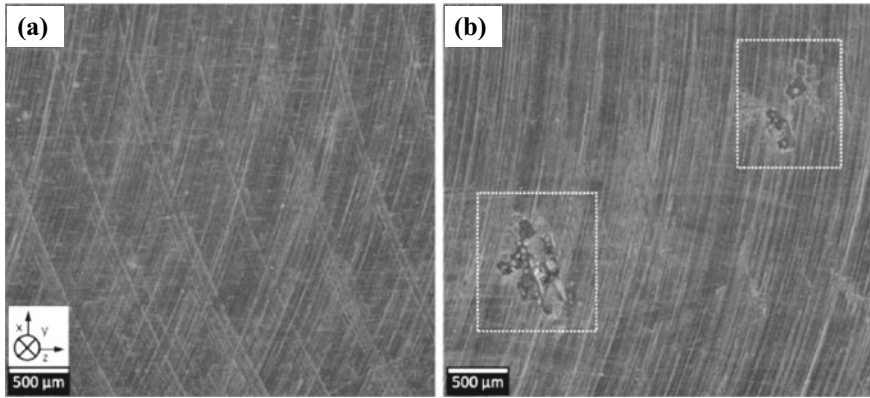
Fig. 8.2 Confocal microscopy images acquired at the surface of EBM Ti6Al4V specimens after FM to a depth of **a** 0.50 mm and; **b** 1.00 mm; dotted squares in (b) highlight defects (Reprinted from, T. Childerhouse et al. [17], with permission from Elsevier)

The extent of decrease in roughness, however, is rather limited (~44–50%). In spite of its ability to remove partially melted powder particles from the surface of the as-built AM part, the impingement of sharp-edged abrasive particles could again cause roughening of the surface. Incorporation of the abrasive particles on the treated surface is a matter of concern. Blasting is considered to be suitable for thick AM parts and it should be used with caution while treating thin lattice structures as impingement of the abrasive particles might damage the part. Zhang [78] have suggested microblasting, which is capable of removing partially melted particles without damaging the part, as a suitable alternative for post-processing of thin lattice structures.

8.2.4 Shot Peening, Cavitation Peening and Laser Shock Peening

Shot peening (SP) involves impingement of a stream of shots on the surface being treated using compressed air. Multiple impingement of the shots enable plastic deformation of the surface and sub-surface, eliminate the surface defects, refine the grains, induce strain hardening, impart compressive residual stress and increase the fatigue resistance [50]. SP facilitated shrinkage of pores and reduced the porosity of SLM AlSi10Mg alloy part by 0.1–0.3%. In addition, SP increased the sphericity of larger pores [18]. SP has been envisioned as a game changer to improve the performance of AM lightweight alloy parts [4]. Unlike SP, cavitation peening (CP) is a shot-less method in which the peening effect is generated by collapsing cavitation bubbles. Similar to SP, CP is also capable of reducing the surface roughness, inducing compressive residual stress and improving the fatigue strength [60].

In laser shock peening (LSP), the shock waves generated by the laser beam induce surface severe plastic deformation (S^2PD), leading to strain hardening, resulting in an increase in hardness along with the formation of a thick hardened layer (~700–900 µm) (Fig. 8.3a) and refines the grain size [16, 31]. LSP changes the tensile residual stress, which is prevalent in LSM metal parts to compressive residual stress (Fig. 8.3b). The choice of a smaller spot size and higher overlap rate (~80%) increase the magnitude of compressive residual stress and the depth to which it is imparted (~900 µm) [35]. The ability of LSP to induce compressive residual stress and to refine the grain size of the α phase helps to reduce the pre-existing crack size, suppress the crack initiation and increase the threshold for fatigue fracture of EBM Ti6Al4V alloy [31]. LSP facilitates a decrease in surface roughness. However, the extent of decrease in roughness of SLM and EBM Ti6Al4V alloy part is relatively less for LSP than SP [33]. Tong et al. [69] have shown that LSP is effective in closing the surface pores (Fig. 8.4) and promoting the formation of a gradient layer structure on DED CoCrFeMnNi high-entropy alloy. According to them, the strength and ductility of the CoCrFeMnNi high-entropy alloy are increased after LSP. The fracture mechanism of CoCrFeMnNi high-entropy alloy and Ti6Al4V alloy is changed to ductile from a mixture of ductile and brittle for as-fabricated part [44, 69].
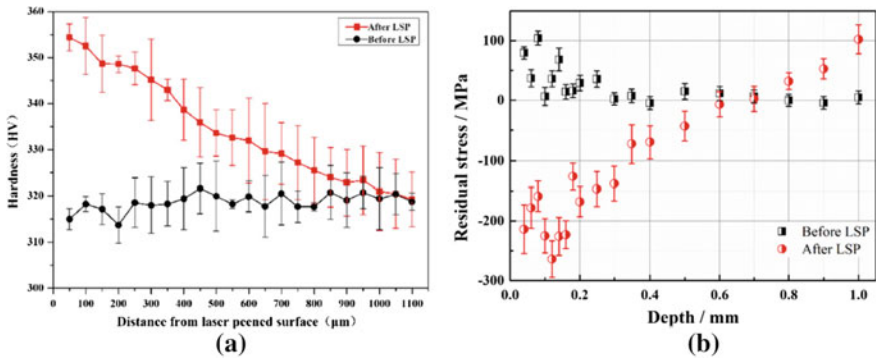
Fig. 8.3 **a** Hardness profile of EBM Ti6Al4V alloy after LSP as a function of depth; and **b** Residual stress of Ti6Al4V alloy as a function of depth before and after LSP (Reprinted from **a** X. Jin et al. [31]; **b** W. Guo et al. [25], with permission from Elsevier)
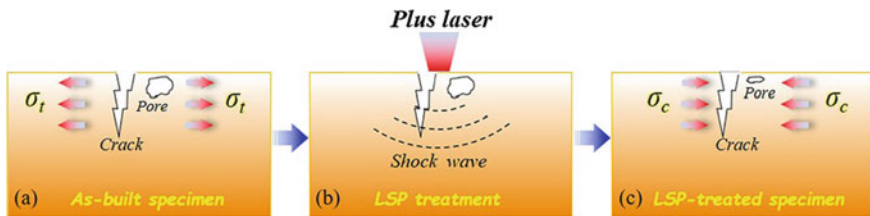

Fig. 8.4 Schematic illustration of closure of surface pores in DED CoCrFeMnNi high-entropy alloy by LSP (Reprinted from Z. Tong et al. [69], with permission from Elsevier)

SLM Ti6Al4V alloy part consists of α'-martensite phase. During SLM, tensile residual stress is induced at the surface of the part. The hardness, YS and UTS of the as-built Ti6Al4V alloy part are higher while it lacks the elongation. Post heat-treatment transformed the α'-martensite phase to α + β phases, decreased the hardness, increased the elongation, released the tensile residual stress, but decreased the YS and UTS. Also, heat-treatment increased the impact toughness, but decreased the corrosion and wear resistance. Yeo et al. [77] have shown that LSP of the heat-treated Ti6Al4V alloy sample has recovered the hardness and wear resistance by about 92% and decreased the corrosion rate by 64%. The ability of LSP to refine the grain size, to increase the magnitude and depth of hardness and, to induce compressive residual stress has enabled an increase in hardness, wear resistance and corrosion resistance of heat-treated SLM Ti6Al4V alloy sample.

Soyama and Takeo [63] have compared the effect of SP, CP and LSP on the extent of decrease in roughness, compressive residual stress induced during peening and increase in fatigue strength of SLM and EBM Ti6Al4V alloy samples. Irrespective of the method of fabrication, the extent of decrease in R_a and R_z by these methods of peening follows the order: SP > CP > LSP while the compressive residual stress induced during peening follows the order: CP > SP > LSP. The increase in fatigue strength after these methods of peening follows the order: CP > CP = LSP for SLM Ti6Al4V alloy and SP > LSP > CP for EBM Ti6Al4V alloy. In terms of fatigue strength, surface roughness exerts a negative influence while compressive residual stress has a positive effect. Sato et al. [60] have shown that the magnitude of compressive residual stress induced during CP of as-built EBM Ti6Al4V alloy is much higher (194 ± 34 MPa) than those induced by SP (127 ± 30 MPa), which is also reflected in the fatigue life. CP has been shown to reduce the microstrain while SP increased the microstrain, which could be the origin of crack initiation. LSP is more expensive when compared to SP and CP [26].

8.2.5 Surface Mechanical Attrition Treatment

Surface mechanical attrition treatment (SMAT) is used as a post-treatment to improve the surface finish of AM metal parts. SMAT is a S^2PD method. The repeated multi-directional impingement of spherical balls on the surface being treated enables plastic deformation, resulting in surface nanocrystallization [7] (Fig. 8.5). During SMAT, plastic deformation of the rough peaks and partially melted particles and subsequent filling of the valleys by the deformed material is responsible for smoothing of the surface [64]. Since plastic deformation is the governing mechanism, the extent of decrease in roughness is dependent on the ductility of the material. SMAT increased the hardness and the strain hardening effect could be realized in the sub-surface region also. SMAT increased the mechanical properties and wear resistance [64]. The compressive residual stress induced by SMAT improves the fatigue performance. Since tensile residual stress dominates on the surface of AM parts, SMAT
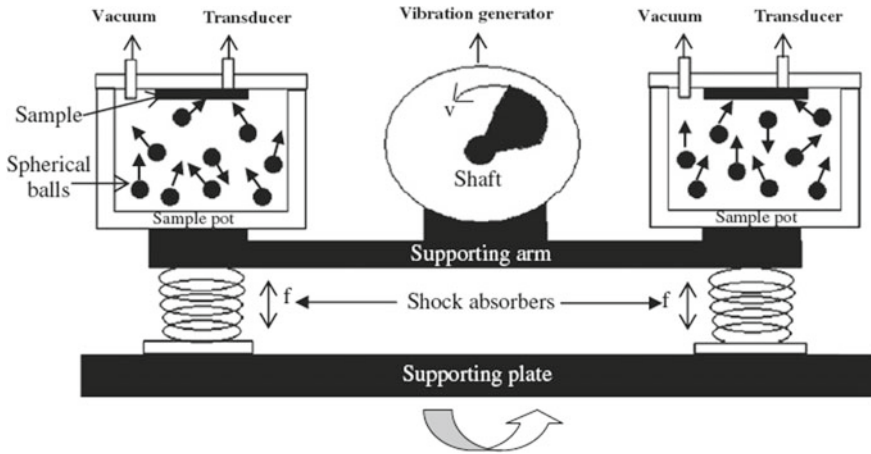
Fig. 8.5 Schematic of the surface mechanical attrition treatment (SMAT) set-up (Reprinted from T. Balusamy et al. [6], with permission from Elsevier)

will be useful to convert it to compressive residual stress [22]. However, SMAT is not amenable for treating AM parts with complex design and internal channels.

8.2.6   Ultrasonic Nanocrystal Surface Modification

Like SMAT, ultrasonic nanocrystal surface modification (UNSM) is also a S^2PD method. UNSM involves repetitive bombardment of a WC tip on the surface being treated at ultrasonic frequencies under a controlled static load (Fig. 8.6a). UNSM
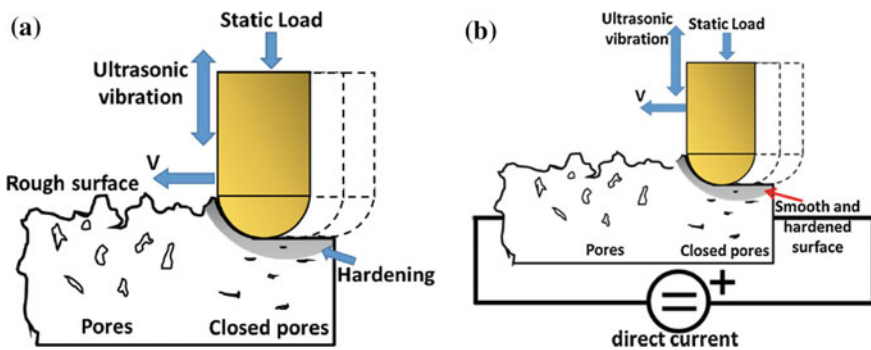
Fig. 8.6 Schematic representation of (a) ultrasonic nanocrystal surface modification (UNSM); and (b) electrically assisted ultrasonic nanocrystal surface modification (EA-UNSM) processes (Reprinted from (a) C. Ma et al. [47]; and (b) H. Zhang et al., [80] with permission from Elsevier)

decreased the surface roughness, improved the surface finish along with the formation of a uniform dimple-like features, decreased the sub-surface porosity, refined the grain size, increased the hardness, converted tensile residual stress to compressive residual stress, improved the fatigue life and increased the corrosion and wear resistance of Ti6Al4V alloy and Ni–Ti alloy [79, 47]. The extent of plastic deformation of SLM 316L SS becomes much higher during UNSM at 400 °C than at 27 °C, which helps to increase the hardness and wear resistance [1]. By an appropriate choice of temperature UNSM can be used to tailor the microstructure of Co-Cr–Mo alloy with a gradient nanostructure (at 25 °C) and a harmonic structure (at 500 °C) [2]. The extent of decrease in surface roughness of AM parts by UNSM is limited. UNSM reduced the elongation of SLM 316L SS from 40 to 24% [1].

Zhang et al. [80] have explored electrically assisted ultrasonic nanocrystal surface modification (EA-UNSM) (Fig. 8.6b) as a post-treatment for 3D printed Ti6Al4V alloy part. When compared to UNSM, the extent of decrease in surface roughness, improvements in surface finish and reduction is surface/sub-surface pores and hardness are much higher in EA-UNSM. The R_a of as-printed Ti6Al4V alloy and those subjected to post-treatment using UNSM and EA-UNSM is 10.6 µm, 7.1 µm and 1.3 µm, respectively. The porosity of the as-printed Ti6Al4V alloy is ~ 1.74%, which is decreased to 1.16% and 0.82% after UNSM and EA-UNSM. The surface hardness of as-printed Ti6Al4V alloy and those subjected to post-treatment using UNSM and EA-UNSM is 359.5 ± 17.3 HV, 437.8 ± 14.2 HV and 484.5 ± 11.9 HV, respectively. Refinement in grain size and strain-hardening are considered responsible for the increase in surface hardness and this effect is much pronounced after EA-UNSM. By an appropriate choice of current density, the temperature can be increased to ~ 425 °C, which enabled a higher extent of plastic deformation. During EA-UNSM, the synergistic mechanical and thermal effect helped to close the surface and sub-surface pores. Materials with plasticity are hard-to-deform. UNSM using a low force is not sufficient to cause plastic deformation while use of a very high force could lead to cracking of the surface/subsurface. On the contrary, the resistive heating during EA-UNSM enables an increase in temperature, which increases the plasticity and facilitates deformation. The easy flow of the rough peak following deformation could offer a better surface finish than those obtained by UNSM.

8.3 Abrasive Finishing Methods

8.3.1 Abrasive Flow Machining

Abrasive flow machining (AFM) was developed by Extrude Hone Corporation to improve the surface finish of internal channels. A viscoelastic medium consisting of abrasive particles pumped at 220 bar enables removal of partially melted particles by micro-cutting and micro-ploughing mechanisms. AFM of SLM Ti6Al4V alloy coupons using a mixture of 60% B_4C, 37% borosiloxane polymer, 2.5% lubricating

grease, and 0.5% oleic acid has reduced the surface roughness from 26 to 0.74 μm [10]. The ability of AFM to reduce both the upskin and downskin surface roughness has been established by [55]. AFM reduced the surface roughness of SLM conformal cooling maraging steel internal channels [27] (Fig. 8.7). In addition, AFM induced compressive residual stress and increased the fatigue strength by 26%. Since the abrasive particles could have limited access in deep valleys, the extent of improvement in fatigue strength becomes limited [27]. Lack of uniform surface finish, particularly at complex bends of internal channels, contamination of the surface with abrasive particles and damage of thin-walled structures at excessive pressures are the major limitations of AFM.
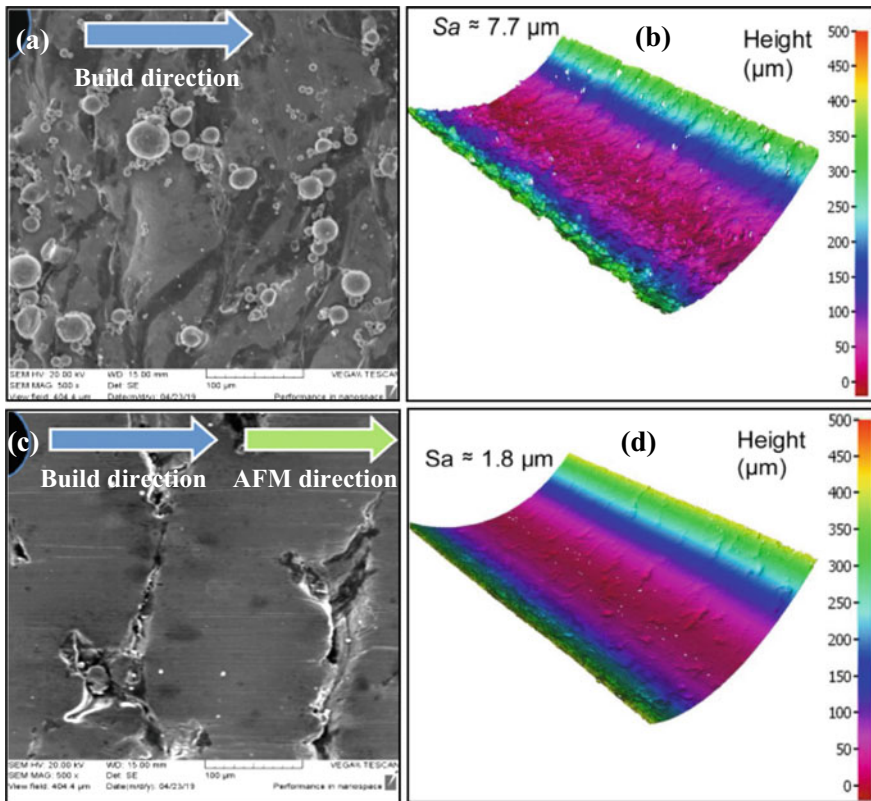
Fig. 8.7 Surface morphology **a**, **c** and 3D surface profile **b**, **d** of SLM conformal cooling maraging steel internal channel: **a**, **b** as-built; **c**, **d** after AFM (Reprinted from S. Han et al. [27], with permission from Elsevier)

8.3.2   Magnetic Field Assisted Abrasive Finish Machining

The difficulty encountered in controlling the cutting force of the abrasive particles in AFM has led to the development of magnetic field assisted abrasive finish machining (MF-AFM) and magnetorheological abrasive flow machining (MR-AFM). The movement of a mixture consisting of abrasive slurry and magnetic particles using an external magnet (NdFeB magnet) enables control of the cutting force of the abrasive particles and limit excessive material removal. Both MF-AFM and MR-AFM can be effectively used to reduce the surface roughness of internal structures of AM parts. Karakurt et al. [34] have shown that MF-AFM using slurries containing SiC and Al_2O_3 is effective in reducing the surface roughness of the external surface of EBM Cu sample from 35 to 4 μm. MF-AFM has been shown to effectively remove all the partially melted particles and balling effect and offer a 76% decrease in surface roughness for SLM 316L SS [81]. MF-AFM performed in three different stages using course, medium and fine particles for 120 min decreased the R_z of SLM 316L SS from 100 to 0.1 μm. However, it involves a material loss of ~ 164 mg with a corresponding decrease in layer thickness by ~ 40 μm.

### 8.3.3   Abrasive Fluidized Bed Machining

Abrasive fluidized bed machining (A-FBM) is based on fluidized bed hydrodynamics in which the hydrodynamic effect created by the air bubbles helps the abrasive particles to impact on the surface of the sample placed inside the fluidized bed [41]. Rotation of the sample inside the fluidized bed promotes interaction between the sample surface and abrasive particles, increases the speed of impingement of abrasive particles and the extent of material removal and thereby improving the process efficiency [21]. Microploughing or microcutting by the abrasive particles is the main mechanism of removal of the partially molten particles. Spherical shaped abrasive particles remove the partially molten particles mainly by microploughing mechanism while both microploughing and microcutting is found to be operative with the use of angular shaped abrasive particles [3]. The cost-effectiveness, ease of automation and sustainability of the process, are the major advantages of A-FBM. Contamination of the surface with abrasive particles, lack of improvement in the surface finish at complex bends of the internal channels are some of the major limitations of A-FBM [41].

8.3.4 Ultrasonic and Hydrodynamic Cavitation Abrasive Finishing

Two types of cavitation abrasive finishing based on ultrasonic and hydrodynamic principles were explored to improve the surface finish of AM parts. Ultrasonic cavitation abrasive finishing (UCAF) involves two different mechanisms: (i) collapse of bubbles on the surface by cavitation; and (ii) impingement of the abrasive particles on the surface. The combined action of both of them offers a decrease in surface roughness. The cavitation bubbles nucleate and grow at the crevices present on the rough as-built AM part subsequently collapse on the surface [65, 66]. Repeated collapse of these bubbles on the surface removes the partially melted powders. Impingement of the abrasive particles accelerated by the cavitation action removes larger-size balls and flattens rough peaks. Use of 1200 grit size micro-abrasive particles is recommended to achieve a good surface finish [65].

In hydrodynamic cavitation abrasive finishing (HCAF), the cavitation bubbles are generated based on hydrodynamic flow principles in which abrasive particles are freely suspended. The partially melted particles present on the surface of the AM part are removed by hydrodynamic cavitation while large-sized balls and rough peaks are removed by the impingement of the abrasive particles accelerated by cavitation [53] (Fig. 8.8).

The bubble-particle interaction that creates a synergistic effect on surface finishing is the unique advantage of HCAF. Due to the synergistic action, HCAF requires only 1% of the abrasive particles as opposed to > 50% of abrasive particles in traditional abrasive finishing methods [53]. The combination of hydrodynamic flow and the use of lower amount of abrasive particles eliminate damage of the corners/edges, thus
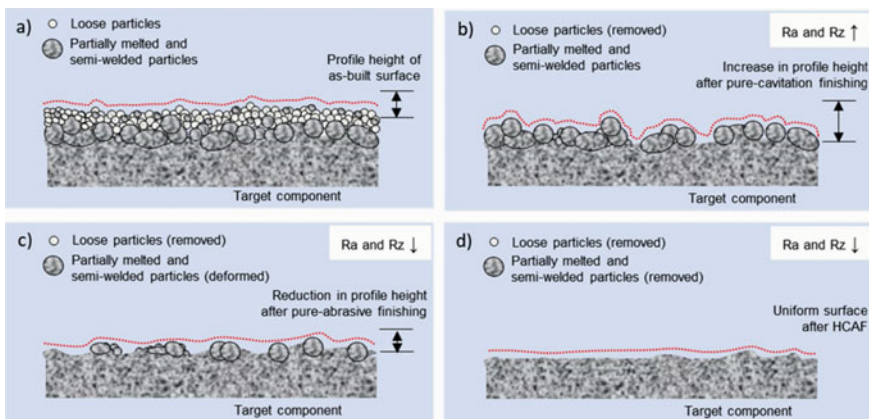
Fig. 8.8 Schematic representation of improvement in surface finishing by HCAF process: **a** as-built AM component surface; **b** after pure-cavitation finishing; **c** after pure-abrasive finishing; and **d** after combined hydrodynamic cavitation abrasive finishing (Reprinted from A.P. Nagalingam, et al. [53], with permission from Elsevier)

preserving the dimensional integrity of the AM part (Fig. 8.9). HCAF is effective in improving the surface finish of internal channels and preserving the circularity of internal contours [52]. HCAF increases the hardness, improves the wetting characteristics, induces compressive residual stress and increases the fatigue life. Erosion of the pump valves with time will be a major concern in HCAF.
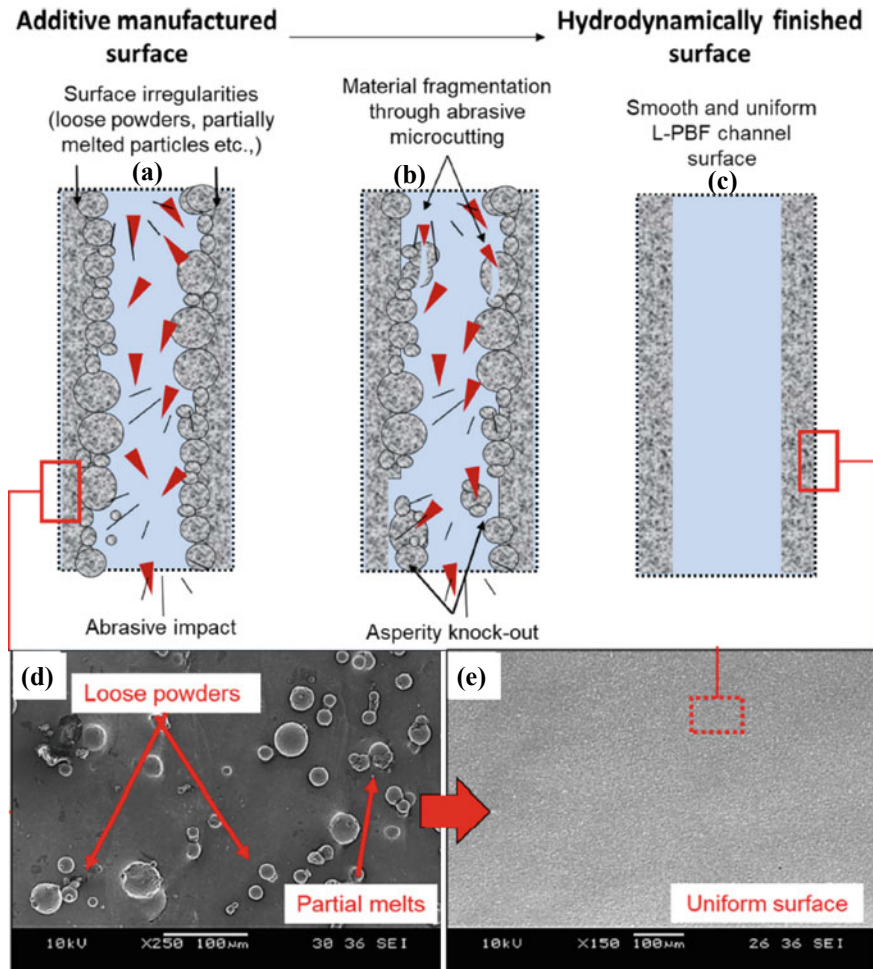
Fig. 8.9 Mechanism of removal of surface irregularities in SLM Inconel 625 alloy internal channels by multi-jet hydrodynamic finishing: **a–c** schematics showing the various stages of material removal and surface smoothening; **d**, **e** surface morphology: **d** as-built internal channel with surface irregularities; and **e** smooth and uniform texture after surface finishing (Reprinted from A.P. Nagalingam and S.H. Yeo, [52] with permission from Elsevier)

8.4 Chemical and Electrochemical Processes

8.4.1 Chemical Etching

Chemical etching (CE) of AM parts involves removal of partially melted particles using acid mixtures. CE of SLM and HIP treated Ti6Al4V alloy part using HF-HNO$_3$-H$_2$O mixture in 1:2:3 ratios for 10 min has enabled a complete removal of partially melted particles, reduced the surface roughness from 12.2 to 6.6 μm, increased the fatigue life, improved the biocompatibility and promoted cellular activity [30]. However, CE decreased the relative density of EBM Ti6Al4V alloy lattice structures following the reduction in strut diameter during CE [19]. SLM CoCr F75 scaffolds become more fragile after CE [73]. Hence, appropriate allowances for the strut thickness and scaffolds should be provided during the design stage itself.

8.4.2 Chemical Polishing

Chemical polishing (CP) involves removal of partially melted powder particles by dissolution using acid mixtures without the requirement for any tools [75]. The difference in rate of dissolution between the peaks and valleys in the AM part enables smoothing of the surface. The gas bubbles formed on the surface keep the dissolution process active without any stagnation. The acid mixtures used for CP is selected based on the type of material. Appropriate dilution of the acid mixtures with longer processing time offers much control during CP while stirring of the polishing solution provides good stability [46]. Unlike mechanical post-treatments, CP concurrently improves the surface finish of both the outer and inner surfaces [70]. CP can be applied to AM parts with complex geometries as well as for thin porous lattice structures and scaffolds (Fig. 8.10). CP is capable of removing irregularities present in AM
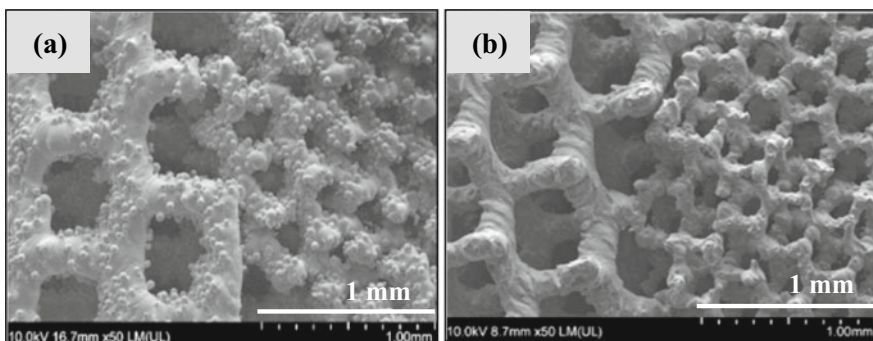
Fig. 8.10 SEM images of the surface of Ti scaffolds: **a** before, **b** after chemical polishing (Reprinted from B. Wysocki et al. [75], with permission from Elsevier)

parts and smoothing of the surface without any change in chemical composition. CP Ti scaffold fails to show any negative effect on the proliferation and growth of MG63 cells, rather it helped to improve colonization [75]. Since the mechanism of eliminating the surface irregularities is by dissolution, mass loss is inevitable during CP. Hence, dimensional integrity of the part after CP is a matter of concern. CP has been shown to decrease the Young's modulus (~ 70%) and compressive strength (~ 30%) [75]. CP is not considered as a suitable choice for post-treating scaffolds with smaller pores.

8.4.3 Combined Chemical and Abrasive Flow Polishing

Mohammadian et al. [51] have shown that the combined chemical abrasive flow polishing using 40 vol. % HF + 40 vol. % HNO_3 + 20 vol. % H_2O dispersed with 420 µm Al_2O_3 particles at a flow velocity of 3 m/s is effective in improving the partially melted particles on the inner surfaces of tubular part made of IN625 alloy, reducing its surface roughness and improving its surface texture. During chemical flow polishing, formation of a passive oxide layer could reduce the rate of polishing. Abrasive flow polishing requires a higher fluid velocity. In combined chemical abrasive flow polishing, the passive oxide layer formed on the surface is continuously removed by the impingement of the abrasive particles.

8.4.4 Electropolishing

Electropolishing (EP) is based on the electrochemically assisted dissolution of the anode under the influence of an applied current and it can be effectively used to improve the surface finish of AM metal parts. Current density is the major factor in determining the efficiency of the EP process. During the initial stages of EP, the residual powders, which protrude outside the surface of the AM part, are removed. Subsequently, polishing of the completed melted layer occurs until the entire surface of the part is uniformly polished (Fig. 8.11). Random dissolution of crystallographic planes during EP is considered responsible for the observed improvement in surface finish [58]. An increase in current density, temperature, treatment time, flow rate, and narrowing the inter-electrode distance would increase the rate of polishing and efficiency. EP is suitable for polishing AM parts with complex shapes, internal channels and thin walled structures, which are usually fragile [71]. EP reduced the contact angle of SLM 316L SS part to 45°, thus making the surface of the part more hydrophilic [70]. The level of surface finish accomplished by EP is much better than those achieved by CP and it is possible to achieve a reduction in surface roughness as high as 92% [71]. Since the average surface roughness (R_a) of SLM Ti6Al4V alloy parts built at different build angles varies from 4 µm (0°) to 23 µm (135°), it is imperative to provide suitable allowance for the current density and time during
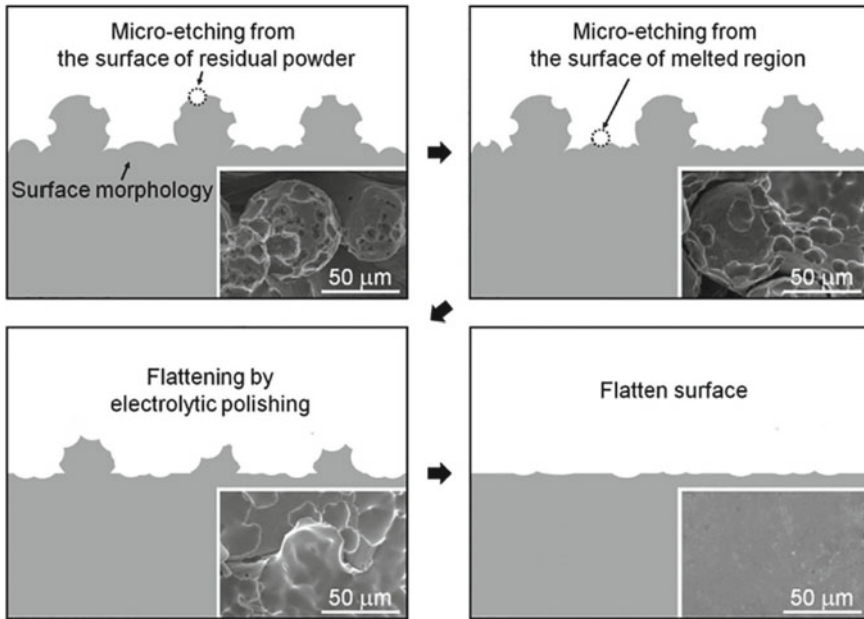
Fig. 8.11 Schematic diagram depicting the mechanism of flattening of surface during EP (Inset: higher magnification images) (Reprinted from J.-H. Jung et al. [32], with permission from Elsevier)

EP to achieve uniform surface finish [71]. The formation of a dense and compact passive oxide layer with fewer defects after EP has increased the corrosion resistance of EMB Ti6Al4V alloy part [74].

The reduction in surface roughness by EP is accompanied a reduction in thickness; the higher the current density, the greater is the extent of polishing and greater is the thickness reduction. For highly rough surfaces, the thickness reduction during EP can be as high as 80 μm, which challenges the dimensional integrity of the AM part [71]. In spite of its ability, the difficulty in placing the cathode within the confined space of internal channels limits the use of EP [70]. EP has been shown to be ineffective in removing holes or cracks or slag present on the surface of the AM part. The presence of an underlying pore in the AM part could promote crack nucleation or crack growth during EP [5, 40]. EP is not effective when the AM part contains non-conducive phases [58]. EP encounters difficulty in polishing multi-phase alloys due to the difference in reactivity of the phases during the electrochemical dissolution process, resulting in an uneven surface finish. The presence of a passive oxide layer such as TiO_2 on the surface of Ti and its alloys poses difficulty during EP and warrants the use of hazardous perchloric ($HClO_4$) and hydrofluoric (HF) acid based electrolytes to remove the passive TiO_2 layer. An increase in duration of EP has been shown to decrease the hardness by 35% and Young's modulus by 45% of SLM Inconel 718 alloy part [5]. Retention of microscopic cavities is a major limitation of EP [70]. Use of an excessive current density for EP has led to the formation of tiny

dots on the surface of EBM Ti6Al4V alloy part, which deleteriously influenced its corrosion resistance in simulated body fluid [74].

8.4.5 Jet Electrochemical Machining

Cheng et al. [15] have suggested jet electrochemical machining (JECM) as a post-treatment method for SLM 316L SS coupons. During JECM, the SLM 316L SS coupon was made as the anode and a nozzle which sprays 10% NaCl was made as the cathode. During JECM, the resistance between the anode and cathode is determined by the electrolyte layer thickness. The higher the thickness, the greater is the resistance. Since the as-built SLM 316L SS coupon is rough, the thickness of the electrolyte layer between the rough peaks (anode) and the nozzle (cathode) is less, which facilitates an easy dissolution of the peaks (Fig. 8.12). During EP as well as in JECM, these peaks assume high current density, which enforces dissolution. Obviously, the rate of metal dissolution will be less at the valleys as the electrolyte layer thickness and the resistance is relatively higher. The surface of SLM 316L SS coupon becomes defect free along with the formation of a microporous structure after JECM at 120 mA/cm^2 for 10 min. The difference in the rate of dissolution at different locations has lead to the development of surface roughness during JECM, resulting in a decrease in roughness only by 53%.
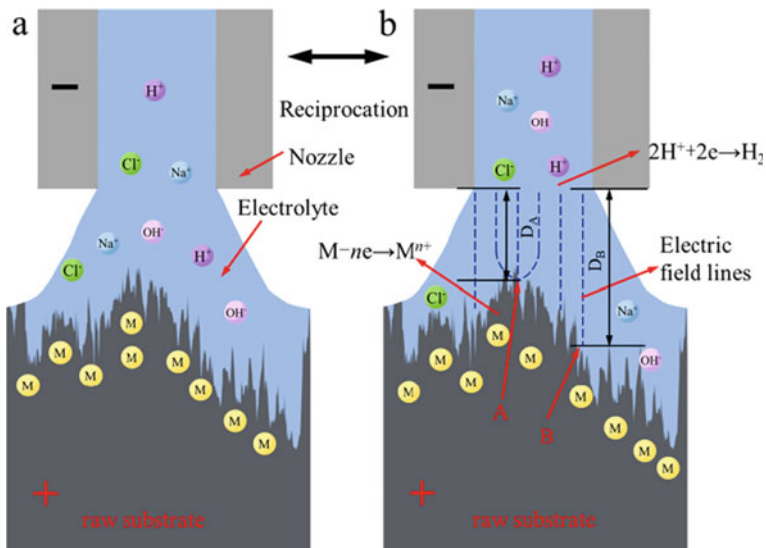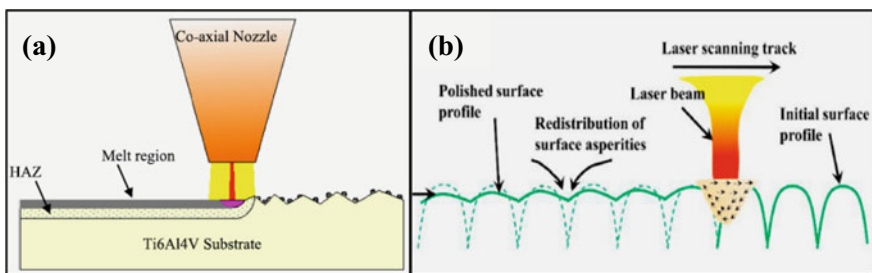

Fig. 8.12 Schematic representation of the JECM: **a** Before JECM; and **b** during JECM (Reprinted from H. Cheng et al. [15], with permission from Elsevier)

8.5 Laser and Electron Beam Processes

8.5.1 Laser Polishing

Laser polishing (LP) involves melting of a thin surface layer and re-distributing the molten layer from the peaks and valleys using the surface tension of the melt, signifying no material removal and only relocation of the molten layer [49, 68] (Fig. 8.13). Hence, dimensional integrity of the component is preserved. The laser energy density, scanning speed, pulse overlap and number of passes are the major factors influencing the process [13, 28]. LP is effective in eliminating the partially melted particles and asperities present in as-built AM part and reconstruct the surface with a smooth finish [13, 14, 42].

The extent of decrease in roughness achieved after LP can be as high as 90–96%. The extent of decrease in surface roughness depends on melt pool velocity. It is imperative to optimize the conditions to achieve a low melt pool velocity which increases the melt pool width rather than the depth [49]. LP refines the grain size, increase the hardness, tensile strength, ductility, fatigue strength, wear resistance and corrosion resistance [13, 14]. LP makes the surface hydrophilic. Repeatability of the process, high speed and ability to polish a selective area are some of the highlights of the process. LP induces tensile residual stress [42, 68]. Crack formation during LP is a major concern [54]. LP is not amenable for surface finishing of internal channels [41]. The choice of a higher laser energy density, insufficient overlap and number of laser passes beyond a threshold has led to an increase in surface roughness [28]. LP promotes surface oxidation in the absence of vacuum or an inert atmosphere [49, 54]. An increase in exposure time during LP extends the HAZ. LP under pulsed mode leads to the formation of porous, cracked surface with an uneven surface oxide layer [23].

Fig. 8.13 Schematic representation of **a** laser polishing; and **b** how the initial surface profile is changed after laser polishing with redistribution of surface asperities (Reprinted from **a** S. Marimuthu et al. [49]; **b** L. Chen et al. [13], with permission from Elsevier)

8.5.2 Laser Re-Melting

Laser remelting improves the surface finish, eliminates the lack of fusion (LOF) pores, decreases the size of the metallurgical pores, increases the density of the part and decreases the residual stress (Fig. 8.14). The rapid solidification after laser remelting refines the grain size. The elimination of pores, decrease in grain size and decrease in residual stress helps to increase the hardness and UTS [36]. The change in surface chemical composition and the thickness of the oxide layer after laser remelting of SLM Ti6Al4V alloy part raises concern on the corrosion resistance and biocompatibility of such parts [72]. The higher cost, decrease in ductility and formation of a thick oxide layer are the major limitations in employing in situ laser remelting.
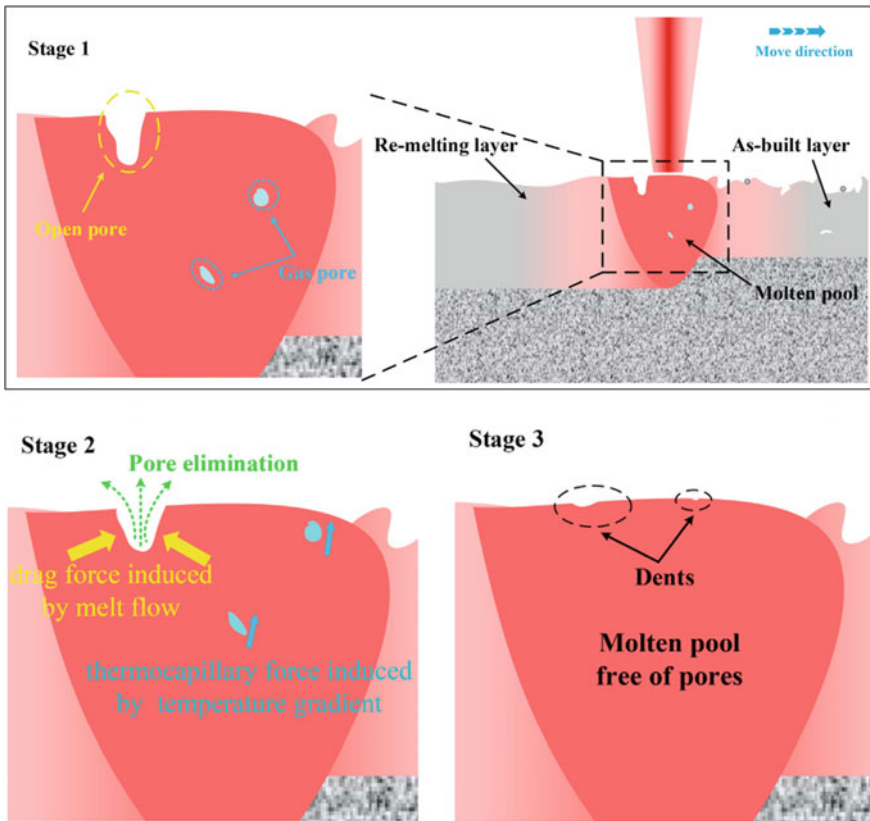
Fig. 8.14 Schematic representation of pore elimination mechanism during laser re-melting process (Reprinted from F. Lv et al. [45], with permission from Elsevier)

8.5.3 Large Pulsed Electron-Beam Irradiation

Large pulsed electron-beam (LPEB) irradiation is similar to LP. Both of them involve melting of the thin surface layer and redistribution of the molten metal pool between the peaks and valleys, resulting in a smooth surface. LPEB irradiation is effective in removing partially melted particles, spatters, cavities, and improving the surface finish [59, 62]. The level of surface finish accomplished after LPEB irradiation is ~ 75% and the treated surfaces are free of microcracks (Fig. 8.15) [59]. LPEB irradiation induces tensile residual stress and involves the formation of a heat affected zone. LPEB irradiation is not suitable for surface finishing of internal channels.

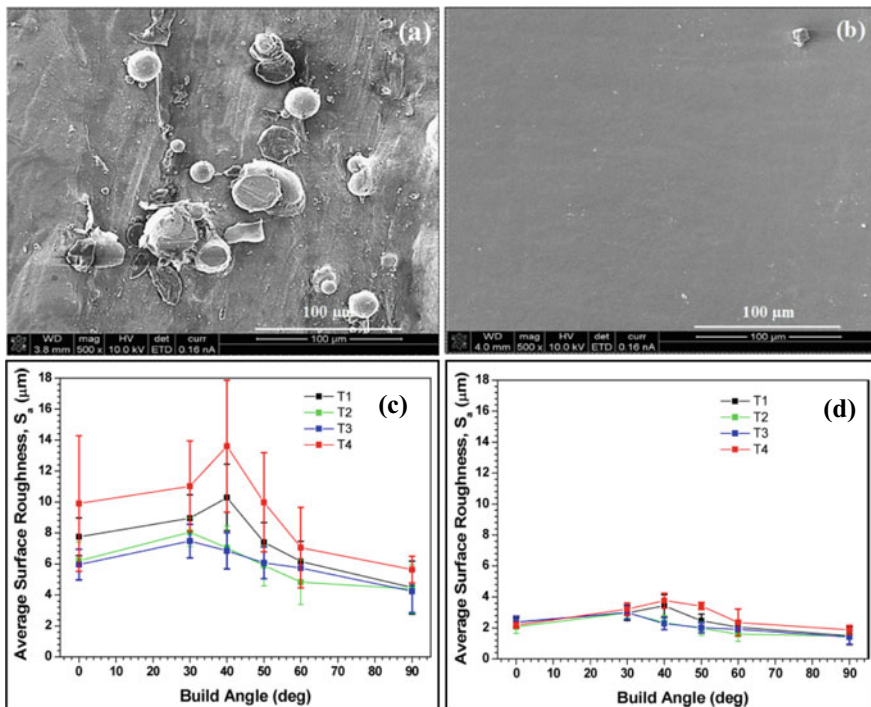**Fig. 8.15 a**, **b** Surface morphology of the uppermost layer of SLM maraging steel samples; and **c**, **d** arithmetical mean height (S_a) of SLM maraging steel samples as a function of build angles: **a**, **c** As-built;; and **b**, **d** after large pulsed electron-beam (LPEB) irradiation; (Reprinted from T.S.N. Sankara Narayanan et al. [59], with permission from Elsevier)

8.6   Hybrid Additive/subtractive Manufacturing

TF could reduce the surface roughness of SLM Ti6Al4V alloy part whereas TF alone could not offer an improvement in fatigue life. SP could induce compressive residual stress and increase the fatigue life. A hybrid treatment of TF and SP has reduced the surface roughness, induced compressive residual stress and increased the fatigue life of SLM.

Ti6Al4V alloy part [20]. The choice of prolonged time duration for TF to decrease the surface roughness and subsequent SP would be cost-effective.

Teng et al. [67] have explored a hybrid treatment involving grinding process (GP) and MAF to decrease the surface roughness of SLM AlSi10Mg alloy. The GP using 160–200 μm sized Al_2O_3 abrasive particles reduced the surface roughness of the as-built AlSi10Mg alloy sample from 7 to 0.6 μm, leaving behind the scratches and pores. The subsequent MAF using spherical SiC W7 magnetic abrasives has reduced the surface roughness from 0.6 to 0.155 μm with a smooth surface finish. The GP induces strain hardening and increased the surface hardness, which is deceased after MAF.

Guo et al. [24] have explored a hybrid treatment of precision grinding (PG) and EP to improve the surface finish of EBM Ti6Al4V alloy part. The R_a as-built part varies from 23–32 μm. EP decreased the R_a to 21–28 μm. PG reduced the R_a to 2 μm, induced compressive residual stress and increased the hardness but it leaves tool marks on the surface. A hybrid treatment of PG followed by EP reduced the R_a to < 1 μm and removed the tool marks. The R_a is decreased further to 0.65 μm when the EP time is increased to 40 min. However, EP released the compressive residual stress induced during PG. Since both PG and EP involves thickness/mass loss, adequate compensation should be provided for the part during the initial design stage.

E-blasting, which combines the unique features of blasting and EP, has been suggested as a hybrid treatment to improve the surface finish of SLM Ti6Al4V alloy part [23]. During E-blasting, the Ti6Al4V alloy part is subjected to EP using a mixture of 700 ml/L of ethyl alcohol + 300 ml/L isopropyl alcohol + 60 g/L AlCl$_3$ + 250 g/L of $ZnCl_2$ and simultaneously blasted using 40–70 μm sized spherical glass beads at a pressure of 5.5 MPa. E-blasting has enabled a clean, smooth and bright surface finish without any defects. Most importantly, the finished surface after E-blasting was free from the blasting media, which is a serious concern in conventional blasting treatment. The level of surface finishing obtained by E-blasting is as high as 92%. E-blasting is effective in reducing the surface roughness of internal cavities.

A hybrid treatment of chemical etching (CE) and electropolishing (EP) using HF based solution has been shown to offer a good reduction in surface roughness of 3D printed Ti6Al4V alloy open porous structure with controlled strut morphology [57]. CE using a mixture of 0.5 ml of 48% HF + 50 g H_2O for 10 min removed the partially melted powders attached to the strut surface. EP using a mixture of 55 ml CH_3COOH + 30 ml H_2SO_4 + 15 ml HF at 1.2 mA/mm^2 for 8 min removed the unevenness and provides a smooth surface finish. However, this hybrid treatment

has increased the internal porosity, decreased the strut thickness and decreased the mechanical properties.

Seo et al. [61] have suggested a hybrid treatment approach of blasting and plasma electrolytic polishing (PEP) to improve the surface finishing of SLM CoCr alloy part. Blasting of the part using stainless steel balls at 7.5 bar reduced the R_a from 13 µm to 3 µm. PEP of the blasted surface using 0.3 M $(NH_4)_2SO_4$ (pH: 5.30; temperature: 75 °C) at 450 V for 8 min has reduced the R_a to 20 nm. The formation of an oxide film on the surface of CoCr alloy after this hybrid treatment has offered an excellent corrosion resistance in 3.5% NaCl.

In situ laser remelting (LR) during fabrication of the part by SLM is a well-known hybrid treatment approach. The SLM-LR hybrid treatment has been shown to eliminate irregular pores and LOF defects, decrease the surface roughness and increase the density of SLM parts [76]. However, this would be possible only with the choice of an appropriate laser power and scanning speed that enables sufficient spreading of the molten material. The choice of a higher laser power for LR provides sufficient time for spreading of the molten material, which reduces the porosity and surface roughness of the top surface. However, the side surface roughness is increased. Although LR at higher laser power reduces the residual stress, it also facilitates the formation of a thick oxide layer, which could affect the mechanical properties of the AM part [8]. During LR at higher laser power, new pores could also be introduced [29]. The choice of a higher scanning speed for LR fails to eliminate the pores whereas a lower scanning speed introduces new pores [45]. LR of each layer after solidification provides a good platform for deposition of the subsequent layer by SLM. The molten layer generated by LR properly wet the underlying solid metal and offer a relatively smooth surface finish [8]. LR decreased the amount of partially melted Ta particles, increased the homogeneity, YS and elastic modulus of the SLM Ti25Ta alloy. However, LR has led to a slight increase in porosity, increased the residual stress, increased the dislocation density, reduced the ductility, decreased the fatigue strength and increased the crack propagation rate of the SLM Ti25Ta alloy. Hence, it is imperative to optimize the conditions employed for LR during the hybrid treatment processes to impart the desired characteristics in the AM part [11].

8.7 Concluding Remarks

A variety of surface finishing post-treatments have been explored to improve the surface finishing of AM metallic components. Each one of them has its own advantages and limitations. The suitability of these methods is ascertained in terms of: (i) Extent of decrease in surface roughness; (ii) thickness/mass loss; (iii) amenability to treat complex design, internal channels and thin lattice structures; (iv) beneficial attributes; (v) problems due to the post-treatment; (vi) process merits in terms of

design aspects, treatment time, selectivity, ability to treat different type of surfaces, wastage and disposal problems and (vii) cost-effectiveness.

(i) Extent of decrease in roughness

The extent of decrease in surface roughness is limited for many mechanical finishing methods. FM could reduce the roughness by 90–96%. Blasting and CE could provide a 50% reduction in roughness. Based on the ability to decrease the surface roughness, peening methods can be ranked as follows: SP > CP > LSP. The level of surface finish accomplished by EP is much better than CP. The reduction in surface roughness can be as high as 92% for EP. Although both CP and EP are capable of treating the internal surfaces of AM parts, CP has an edge over EP due to the difficulty in placing the counter electrode in the latter case. The extent of decrease in roughness achieved after LP can be as high as 90–96% while LPEB irradiation offers ~ 75% reduction in surface roughness.

(ii) Thickness/mass loss

Mechanical surface finishing methods obviously involve thickness/mass loss. The extent of thickness/mass loss is much higher in CP and EP. The thickness reduction during EP can be as high as 80 μm. Hence, dimensional integrity of the AM part after CP and EP is a matter of concern. LP and LPEB irradiation involve no material removal and the molten material is redistributed between the peaks and valleys, resulting in a smooth surface. Hence, dimensional integrity of the AM component is preserved.

(iii) Amenability to treat complex design, internal channels and thin lattice structures

TF/BF is amenable for treating AM parts with complex shapes with limited improvement in surface finish. Blasting is considered to be suitable for treating thick AM parts. Internal channels can be treated with limited success. However, impingement of the abrasive particles might damage thin lattice structures. Abrasive finishing methods are effective in treating internal channels. CP and EP are suitable for treating AM parts with complex geometries, internal channels and fragile thin walled structures. FM, LP, LPEB irradiation, SMAT and UNSM are not amenable for treating AM parts with complex shapes and internal channels.

(iv) Beneficial attributes

SP, CP, LSP, SMAT and UNSM reduce the surface roughness by plastic deformation. The compressive residual stress induced during these methods helps to increase the fatigue strength of the AM part. CP, EP and LP provide a highly polished surface, decrease the contact angle and make the finished surface more hydrophilic. Such surfaces could increase the biocompatibility and promote cell proliferation and growth. Repeatability, high speed and ability to polish a selective area are some of the highlights of LP.

(v) Problems imposed by the post-treatment methods

Blasting leads to incorporation of abrasive particles on the treated surface. CE reduced the strut diameter and decreased the relative density of lattice structures. Moreover, CE makes the scaffolds fragile. Prolonged use of SP is not effective in reducing the surface roughness. CP decreased the Young's modulus and compressive strength of AM part. EP decreased the hardness and Young's modulus. Both CP and EP retain microscopic cavities. Use of an excessive current density for EP induced pitting on the surface and deleteriously influenced the corrosion resistance. LP induces tensile residual stress. Crack formation during LP is a major concern. LP promotes surface oxidation when performed in the absence of vacuum or an inert atmosphere. An increase in exposure time during LP extends the HAZ. LP under pulsed mode results in the formation of a porous, cracked surface with an uneven surface oxide layer. LPEB irradiation induces tensile residual stress and involves the formation of a heat affected zone.

(vi) Process merits in terms of design aspects, treatment time, selectivity, ability to treat different type of surfaces, wastage and disposal problems

Many mechanical methods such as TF/BF, DF, VSF, etc. require a longer processing time to decrease the surface roughness. On the contrary, FM, SP, LP and EP could reduce the surface roughness at a shorter duration of time. Wastage of the abrasive media and problems in disposing them are the major limitations in TF/BF as well as in abrasive finishing methods. CE, CP, EP involves immersion of the whole AM part in the electrolyte, pointing out the lack of selectivity. Disposal of spent acids is a serious concern in CE, CP and EP. Designing cathodes according to the geometry of the AM and the difficulty in placing the cathode within a confined space of internal channels are other major process limitations in EP. The difficulty encountered in treating AM parts with multi-phase alloys, non-conductive phases and slags is yet another challenge in EP. The choice of a higher laser energy density, insufficient overlap and number of laser passes beyond a threshold has increased the surface roughness in LP.

(vii) Cost-effectiveness

Mechanical surface finishing methods are cost-effective. Abrasive finishing methods and chemical and electrochemical methods involve a moderate cost. Laser based processes such as LP and LSP as well as LPEB irradiation are expensive.

Regarding the choice of post-treatment for AM part, "one solution for all" is not possible. The appropriate method should be chosen based on the type of AM part, its complexity, thickness, fragility, type of phase present and the end use of the part. If fatigue strength of the part is important, then peening methods might be a good choice. For treating internal channels, abrasive finishing methods are the most appropriate choice. Many hybrid treatment methods are also being explored. For many parts, a suitable combination of two or three methods of surface post-treatment under optimized conditions would offer a good surface finish. The quest for a better surface finishing post-treatment for AM parts continues.

8.8 Future Perspectives

The role of surface finishing post-treatments to improve the surface finish of metals and alloys are addressed in this chapter. Many hybrid treatments are emerging, which extends the window of opportunity of achieving a better surface finish for metals and alloys. Recently, the realm of AM extends beyond metals and alloys. Bimetallic materials, composites and functionally graded materials are fabricated by AM. In addition, AM of components with multi-materials such as metal–metal, metal-ceramic and metal-polymeric are being explored for numerous applications. The surface finishing post-treatment methods and conditions employed for metals and alloys cannot be used as such for the emerging bimetallic materials, composites, functionally graded materials and multi-material systems. To realize the fullest potential of AM of emerging materials, suitable modifications have to be proposed in the surface finishing methods to accommodate the emerging materials. The functionally graded materials and multi-material systems warrant the development of new methods of surface finishing. Much remains to be explored in this area. Surface engineering/modification research will again assume significance as many new developments are made in AM.

References

1. Amanov, A.: Effect of local treatment temperature of ultrasonic nanocrystalline surface modification on tribological behavior and corrosion resistance of stainless steel 316L produced by selective laser melting. Surf. Coat. Technol. **398**, 126080 (2020a)
2. Amanov, A.: A promising post-additive manufacturing surface modification for tailoring gradient nanostructure and harmonic structure in Co-Cr-Mo alloy. Vacuum **182**, 109702 (2020b)
3. Atzeni, E., Barletta, M., Calignano, F., Iuliano, L., Rubino, G., Tagliaferri, V.: Abrasive fluidized bed (AFB) finishing of AlSi10Mg substrates manufactured by direct metal laser sintering (DMLS). Addit. Manuf. **10**, 15–23 (2016)
4. Bagherifard, S.: Enhancing the structural performance of lightweight metals by shot peening. Adv. Eng. Mater. **21**, 1801140 (2019)
5. Baicheng, Z., Xiaohua, L., Jiaming, B., Junfeng, G., Pan, W., Chen-nan, S., Muiling. N., Guojun, Q., Jun, W.: Study of selective laser melting (SLM) Inconel 718 part surface improvement by electrochemical polishing. Mater. Des. **116**, 531–537 (2017)
6. Balusamy, T., Kumar, S., Sankara Narayanan, T.S.N.: Effect of surface nanocrystallization on the corrosion behaviour of AISI 409 stainless steel. Corros. Sci. **52**(11), 3826–3834 (2010)
7. Balusamy, T., Sankara Narayanan, T.S.N. and Park, H.Y.: Surface Nanostructuring of Metallic Materials for Implant Applications. In: Santra, T.S. Mohan, L. (Eds.) Nanomaterials and Their Biomedical Applications, pp. 465–511. Springer, Singapore (2021)
8. Bayati, P., Safaei, K., Nematollahi, M., Jahadakbar, A., Yadollahi, A., Mahtabi, M., Elahinia, M.: Toward understanding the effect of remelting on the additively manufactured NiTi. Int. J. Adv. Manuf. Technol. **112**, 347–360 (2021)
9. Boschetto, A., Bottini, L., Macera, L., Veniali, F.: Post-processing of complex SLM parts by Barrel Finishing. Appl. Sci. **10**, 1382 (2020)
10. Bouland, C., Urlea, V., Beaubier, K., Samoilenko, M., Brailovski, V.: Abrasive flow machining of laser powder bed-fused parts: Numerical modeling and experimental validation. J. Mater. Process. Technol. **273**, 116262 (2019)

11. Brodie, E.G., Richter, J., Wegener, T., Niendorf, T., Molotnikov, A.: Low-cycle fatigue performance of remelted laser powder bed fusion (L-PBF) biomedical Ti25Ta. Mater. Sci. Eng. A **798**, 140228 (2020)
12. Chen, Z., Wu, X., Tomus, D., Davies, C.H.J.: Surface roughness of selective laser melted Ti-6Al-4V alloy components. Addit. Manuf. **21**, 91–103 (2018)
13. Chen, L., Richter, B., Zhang, X., Ren, X., Pfefferkorn, F.E.: Modification of surface characteristics and electrochemical corrosion behavior of laser powder bed fused stainless-steel 316L after laser polishing. Addit. Manuf. **32**, 101013 (2020)
14. Chen, L., Richter, B., Zhang, X., Bertsch, K.B., Thoma, D.J., Pfefferkorn, F.E.: Effect of laser polishing on the microstructure and mechanical properties of stainless steel 316L fabricated by laser powder bed fusion. Mater. Sci. Eng. A **802**, 140579 (2021)
15. Cheng, H., Xu, B., Xie, D., Yang, Y., Shen, L., Qiu, M., Chen, Y., Lou, G., Zhao, J., Tian, Z.: Improvement of selective laser melting substrate surface performance via combined processing of jet electrochemical machining and jet electrodeposition. Surf. Coat. Technol. **412**, 127028 (2021)
16. Chi, J., Cai, Z., Zhang, H., Zhang, H., Guo, W., Wan, Z., Han, G., Peng, P., Zeng, Z.: Combining manufacturing of titanium alloy through direct energy deposition and laser shock peening processes. Mater. Des. **203**, 109626 (2021)
17. Childerhouse, T., Hernandez-Nava, E., M'Saoubi, R., Tapoglou, N., Jackson, M.: Surface and sub-surface integrity of Ti-6Al-4V components produced by selective electron beam melting with post-build finish machining. Procedia CIRP **87**, 309–314 (2020)
18. Damon, J., Dietrich, S., Vollert, F., Gibmeier, J., Schulze, V.: Process dependent porosity and the influence of shot peening on porosity morphology regarding selective laser melted AlSi10Mg parts. Addit. Manuf. **20**, 77–89 (2018)
19. de Formanoir, C., Suard, M., Dendievel, R., Martin, G., Godet, S.: Improving the mechanical efficiency of electron beam melted titanium lattice structures by chemical etching. Addit. Manuf. **11**, 71–76 (2016)
20. Denti, L., Bassoli, E., Gatto, A., Santecchia, E., Mengucci, P.: Fatigue life and microstructure of additive manufactured Ti6Al4V after different finishing processes. Mater. Sci. Eng. A. **755**, 1–9 (2019)
21. El Hassanin, A., Troiano, M., Scherillo, F., Silvestri, A.T., Contaldi, V., Solimene, R., Scala, F., Squillace, A., Salatino, P.: Rotation-assisted abrasive fluidised bed machining of AlSi10Mg parts made through selective laser melting technology. Procedia Manuf. **47**, 1043–1049 (2020)
22. Eyzat, Y., Chemkhi, M., Portella, Q., Gardan, J., Remond, J., Retraint, D.: Characterization and mechanical properties of as-built SLM Ti-6Al-4V subjected to surface mechanical post-treatment. Procedia CIRP **81**, 1225–1229 (2019)
23. García-Blanco, M.B., Díaz-Fuentes, M., Espinosa, E., Mancisidor, A.M., Vara, G.: Comparative study of different surface treatments applied to Ti6Al4V parts produced by Selective Laser Melting. Trans. Inst. Met. Finish. (2021). https://doi.org/10.1080/00202967.2021.1898171
24. Guo, J., Goh, M.H., Wang, P., Huang, R., Lee, X., Wang, B., Nai, S.M.L., Wei, J.: Investigation on surface integrity of electron beam melted Ti-6Al-4V by precision grinding and electropolishing. Chinese J. Aeronaut. Available online 2 Sept 2020. https://doi.org/10.1016/j.cja.2020.08.014
25. Guo, W., Sun, R., Song, B., Zhu, Y., Li, F., Che, Z., Li, B., Peng, P.: Laser shock peening of laser additive manufactured Ti6Al4V titanium alloy. Surf. Coat. Technol. **349**, 503–510 (2018)
26. Hackel, L., Rankin, J.R., Rubenchik, A., King, W.E., Matthews, M.: Laser peening: A tool for additive manufacturing post-processing. Addit. Manuf. **24**, 67–75 (2018)
27. Han, S., Salvatore, F., Rech, J., Bajolet, J., Courbon, J.: Effect of abrasive flow machining (AFM) finish of selective laser melting (SLM) internal channels on fatigue performance. J. Manuf. Process. **59**, 248–257 (2020)
28. Hofele, M., Schanz, J., Roth, A., Harrison, D.K., De Silva, A.K.M., Riegel, H.: Process parameter dependencies of continuous and pulsed laser modes on surface polishing of additive manufactured aluminium AlSi10Mg parts. Mater. Sci. Eng. Technol. (Materialwiss. Werkstofftech) **52**(4), 409–432 (2021)

29. Hu, Z., Nagarajan, B., Song, X., Huang, R., Zhai, W., Wei, J.: Tailoring surface roughness of micro selective laser melted SS316L by In-Situ Laser Remelting. In: Itoh, S., Shukla, S. (eds.) INCASE 2019, LNME, pp. 337–343, Springer, Singapore Pte Ltd. (2020)
30. Jamshidi, P., Aristizabal, M., Kong, W., Villapun, V., Cox, S.C., Grover, L.M., Attallah, M.M.: Selective laser melting of Ti-6Al-4V: The impact of post-processing on the Tensile, Fatigue and biological properties for medical implant applications. Materials **13**(12), 2813 (2020)
31. Jin, X., Lan, L., Gao, S., He, B., Rong, Y.: Effects of laser shock peening on microstructure and fatigue behavior of Ti-6Al-4V alloy fabricated via electron beam melting. Mater. Sci. Eng. A. **780**, 139199 (2020)
32. Jung, J.-H., Park, H.-K., Lee, B.S., Choi, J., Seo, B., Kim, H.K., Kim, H.G., Kim, H.G.: Study on surface shape control of pure Ti fabricated by electron beam melting using electrolytic polishing. Surf. Coat. Technol. **324**, 106–110 (2017)
33. Kahlin, M., Ansell, H., Kerwin, A., Smith, B., Moverare, J.: Variable amplitude loading of additively manufactured Ti6Al4V subjected to surface post processes. Int. J. Fatigue **142**, 105945 (2021)
34. Karakurt, I., Ho, K.Y., Ledford, C., Gamzina, D., Horn, T., Luhmann, N.C., Lin, L.: Development of a magnetically driven abrasive polishing process for additively manufactured copper structures. Procedia Manuf. **26**, 798–805 (2018)
35. Kalentics, N., Boillat, E., Peyre, P., Gorny, C., Kenel, C., Leinenbach, C., Jhabval, J., Logé, R.E.: 3D Laser shock peening—A new method for the 3D control of residual stresses in Selective Laser Melting. Mater. Des. **130**, 350–356 (2017)
36. Karimi, J., Suryanarayana, C., Okulov, I., Prashanth, K.G.: Selective laser melting of Ti6Al4V: Effect of laser re-melting. Mater. Sci. Eng. A **805**, 140558 (2020)
37. Kaynak, Y., Kitay, O.: Porosity, surface quality, microhardness and microstructure of selective laser melted 316L stainless steel resulting from finish machining. J. Manuf. Mater. Process. **2**(2), 36 (2018)
38. Kaynak, Y., Kitay, O.: The effect of post-processing operations on surface characteristics of 316L stainless steel produced by selective laser melting. Addit. Manuf. **26**, 84–93 (2019)
39. Kaynak, Y., Tascioglu, E.: Post-processing effects on the surface characteristics of Inconel 718 alloy fabricated by selective laser melting additive manufacturing. Prog. Addit. Manuf. **5**, 221–234 (2020)
40. Khan, H.M., Karabulut, Y., Kitay, O., Kaynak, Y., Jawahir, I.S.: Influence of the post-processing operations on surface integrity of metal components produced by laser powder bed fusion additive manufacturing: A review. Mach. Sci. Technol. **25**(1), 118–176 (2021)
41. Lee, J.-Y., Nagalingam, A.P., Yeo, S.H.: A review on the state-of-the-art of surface finishing processes and related ISO/ASTM standards for metal additive manufactured components. Virtual Phys. Prototyp. **16**(1), 68–96 (2021)
42. Lee, S., Ahmadi, Z., Pegues, J.W., Mahjouri-Samani, M., Shamsaei, N.: Laser polishing for improving fatigue performance of additive manufactured Ti-6Al-4V parts, Opt. Laser Technol. **134**, 106639 (2021b)
43. Liu, S., Shin, Y.C.: Additive manufacturing of Ti6Al4V alloy: A review. Mater. Des. **164**, 107552 (2019)
44. Lu, J., Lu, H., Xu, X., Yao, J., Cai, J., Luo, K.: High-performance integrated additive manufacturing with laser shock peening induced microstructural evolution and improvement in mechanical properties of Ti6Al4V alloy components. Int. J. Mach. Tools Manuf. **148**, 103475 (2019)
45. Lv, F., Liang, H., Xie, D., Mao, Y., Wang, C., Shen, L., Tian, Z.: On the role of laser in situ re-melting into pore elimination of Ti6Al4V components fabricated by selective laser melting. J. Alloys Compd. **854**, 156866 (2021)
46. Łyczkowska, E., Szymczyk, P., Dybała, B., Chlebus, E.: Chemical polishing of scaffolds made of Ti-6Al-7Nb alloy by additive manufacturing. Arch. Civ. Mech. Eng. **14**, 586–594 (2014)
47. Ma, C., Andani, M.T., Qin, H., Moghaddam, N.S., Ibrahim, H., Jahadakbar, A., Amerinatanzi, A., Ren, Z., Zhang, H., Doll, G.L., Dong, Y., Elahinia, M., Ye, C.: Improving surface finish and wear resistance of additive manufactured nickel-titanium by ultrasonic nano-crystal surface modification. J. Mater. Process. Technol. **249**, 433–440 (2017)

48. Maleki, E., Bagherifard, S., Bandini, M., Guagliano, M.: Surface post-treatments for metal additive manufacturing: Progress, challenges, and opportunities. Addit. Manuf. **37**, 101619 (2021)
49. Marimuthu, S., Triantaphyllou, A., Antar, M., Wimpenny, D., Morton, H., Beard, M.: Laser polishing of selective laser melted components. Int. J. Mach. Tools Manuf. **95**, 97–104 (2015)
50. Maamoun, A., Elbestawi, M., Veldhuis, S.: Influence of shot peening on AlSi10Mg parts fabricated by additive manufacturing. J. Manuf. Mater. Process. **2**(3), 40 (2018)
51. Mohammadian, N., Turenne, S., Brailovski, V.: Surface finish control of additively-manufactured Inconel 625 components using combined chemical-abrasive flow polishing. J. Mater. Process. Technol. **252**, 728–738 (2018)
52. Nagalingam, A.P., Yeo, S.H.: Surface finishing of additively manufactured Inconel 625 complex internal channels: A case study using a multi-jet hydrodynamic approach. Addit. Manuf. **36**, 101428 (2020)
53. Nagalingam, A.P., Yuvaraj, H.K., Yeo, S.H.: Synergistic effects in hydrodynamic cavitation abrasive finishing for internal surface-finish enhancement of additive-manufactured components. Addit. Manuf. **33**, 101110 (2020)
54. Nesli, S., Yilmaz, O.: Surface characteristics of laser polished Ti-6Al-4V parts produced by electron beam melting additive manufacturing process. Int. J. Adv. Manuf. Technol. **114**, 271–289 (2021)
55. Peng, C., Fu, Y., Wei, H., Li, S., Wang, X., Gao, H.: Study on improvement of surface roughness and induced residual stress for additively manufactured metal parts by abrasive flow machining. Procedia CIRP **71**, 386–389 (2018)
56. Peng, X., Kong, L., Fuh, J.Y.H., Wang, H.: A review of post-processing technologies in additive manufacturing. J. Manuf. Mater. Process. **5**(2), 38 (2021)
57. Pyka, G., Burakowski, A., Kerckhofs, G., Moesen, M., Van Bael, S., Schrooten, J., Wevers, M.: Surface modification of Ti6Al4V open porous structures produced by additive manufacturing. Adv. Eng. Mater. **14**(6), 363–370 (2012)
58. Rotty, C., Doche, M.-L., Mandroyan, A., Hihn, J.-Y., Montavon, G., Moutarlier, V.: Comparison of electropolishing behaviours of TSC, ALM and cast 316L stainless steel in H_3PO_4/H_2SO_4. Surf. Interfaces **6**, 170–176 (2017)
59. Sankara Narayanan, T.S.N., Kim, J., Jeong, H.E., Park, H.W.: Enhancement of the surface properties of selective laser melted maraging steel by large pulsed electron-beam irradiation. Addit. Manuf. **33**, 101125 (2020)
60. Sato, M., Takakuwa, O., Nakai, M., Niinomi, M., Takeo, F., Soyama, H.: Using cavitation peening to improve the fatigue life of titanium alloy Ti-6Al-4V manufactured by electron beam melting. Mater. Sci. Appl. **7**, 181–191 (2016)
61. Seo, B., Park, H.-K., Kim, H. G., Kim, W. R., Park, K.: Corrosion behavior of additive manufactured CoCr parts polished with plasma electrolytic polishing. Surf. Coat. Technol. **406**, 126640 (2021)
62. Shinonaga, T., Yamaguchi, A., Okamoto, Y., Okada(1), A.: Surface smoothing and repairing of additively manufactured metal products by large-area electron beam irradiation, CIRP Annals, IN Press, Available online 13 May 2021 (2021). https://doi.org/10.1016/j.cirp.2021.04.063
63. Soyama, H., Takeo, F.: Effect of various peening methods on the fatigue properties of titanium alloy Ti6Al4V manufactured by direct metal laser sintering and electron beam melting. Materials **13**, 2216 (2020)
64. Sun, Y., Bailey, R., Moroz, A.: Surface finish and properties enhancement of selective laser melted 316L stainless steel by surface mechanical attrition treatment. Surf. Coat. Technol. **378**, 124993 (2019)
65. Tan, K.L., Yeo, S.H.: Surface modification of additive manufactured components by ultrasonic cavitation abrasive finishing. Wear **378–379**, 90–95 (2017)
66. Tan, K.L., Yeo, S.H.: Surface finishing on IN625 additively manufactured surfaces by combined ultrasonic cavitation and abrasion. Addit. Manuf. **31**, 100938 (2020)
67. Teng, X., Zhang, G., Zhao, Y., Cui, Y., Li, L., Jiang, L.: Study on magnetic abrasive finishing of AlSi10Mg alloy prepared by selective laser melting. Int. J. Adv. Manuf. Technol. **105**, 2513–2521 (2019)

68. Tian, Y., Gora, W.S., Cabo, A.P., Parimi, L.L., Hand, D.P., Tammas-Williams, S., Prangnell, P.B.: Material interactions in laser polishing powder bed additive manufactured Ti6Al4V components. Addit. Manuf. **20**, 11–22 (2018)
69. Tong, Z., Liu, H., Jiao, J., Zhou, W., Yang, Y., Ren, X.: Improving the strength and ductility of laser directed energy deposited CrMnFeCoNi high-entropy alloy by laser shock peening. Addit. Manuf. **35**, 101417 (2020)
70. Tyagi, P., Goulet, T., Riso, C., Stephenson, R., Chuenprateep, N., Schlitzer, J., Benton, C., Garcia-Moreno, F.: Reducing the roughness of internal surface of an additive manufacturing produced 316 steel component by chempolishing and electropolishing. Addit. Manuf. **25**, 32–38 (2019)
71. Urlea, V., Brailovski, V.: Electropolishing and electropolishing-related allowances for powder bed selectively laser-melted Ti-6Al-4V alloy components. J. Mater. Process. Technol. **242**, 1–11 (2017)
72. Vaithilingam, J., Goodridge, R.D., Hague, R.J.M., Christie, S.D.R., Edmondson, S.: The effect of laser remelting on the surface chemistry of Ti6al4V components fabricated by selective laser melting. J. Mater. Process. Technol. **232**, 1–8 (2016)
73. van Hooreweder, B., Lietaert, K., Neirinck, B., Lippiatt, N., Wevers, M.: CoCr F75 scaffolds produced by additive manufacturing: influence of chemical etching on powder removal and mechanical performance. J. Mech. Behav. Biomed. Mater. **70**, 60–67 (2017)
74. Wu, Y.-C., Kuo, C.-N., Chung, Y.-C., Ng, C.-H., Huang, J.C.: Effects of electropolishing on mechanical properties and bio-corrosion of Ti6Al4V fabricated by electron beam melting additive manufacturing. Materials **12**(9), 1466 (2019)
75. Wysocki, B., Idaszek, J., Buhagiar, J., Szlązak, K., Brynk, T., Kurzydłowski, K.J., Święszkowski, W.: The influence of chemical polishing of titanium scaffolds on their mechanical strength and in-vitro cell response. Mater. Sci. Eng. C. **95**, 428–439 (2019)
76. Yasa, E., Deckers, J., Kruth, J.: The investigation of the influence of laser re-melting on density, surface quality and microstructure of selective laser melting parts. Rapid Prototyp. J. **17**(5), 312–327 (2011)
77. Yeo, I., Bae, S., Amanov, A., Jeong, S.: Effect of laser shock peening on properties of heat-treated Ti-6Al-4V manufactured by laser powder bed fusion. Int. J. Precis. Eng. Manuf.-Green Tech. (2020). https://doi.org/10.1007/s40684-020-00234-2
78. Zhang, J.: Micro-blasting of 316L tubular lattice manufactured by laser powder bed fusion. In: Proceedings of the 19th International Conference of the European Society For Precision Engineering and Nanotechnology EUSPEN 2019, Bilbao, Spain, 3–7 June 2019
79. Zhang, H., Chiang, R., Qin, H., Ren, Z., Hou, X., Lin, D., Doll, G.L., Vasudevan, V.K., Dong, Y., Ye, C.: The effects of ultrasonic nanocrystal surface modification on the fatigue performance of 3D-printed Ti64. Int. J. Fatigue **103**, 136–146 (2017)
80. Zhang, H., Zhao, J., Liu, J., Qin, H., Ren, Z., Doll, G.L., Dong, Y., Ye, C.: The effects of electrically-assisted ultrasonic nanocrystal surface modification on 3D-printed Ti-6Al-4V alloy. Addit. Manuf. **22**, 60–68 (2018)
81. Zhang, J., Chaudhari, A., Wang, H.: Surface quality and material removal in magnetic abrasive finishing of selective laser melted 316L stainless steel. J. Manuf. Process. **45**, 710–719 (2019)